Modeling carbon sequestration in the subsoil and the time required to stabilize carbon at timescales relevant for climate change mitigation *

Carlos A. Sierra Martin Bolinder Maarten C. Braakhekke Sophie von Fromm
Thomas Kätterer Zhongkui Luo Nargish Parvin Guocheng Wang

April 19, 2023

Abstract

Soils store large quantities of carbon in the subsoil that is generally old and believed to be stabilized over centuries to millennia, which suggests that subsoil carbon sequestration can be used as a powerful strategy for climate change mitigation. In this contribution, we review the main biophysical processes that contribute to carbon storage in subsoil and the main mathematical models used to represent these processes. Our guiding objective is to review whether a process understanding of soil C movement in the vertical profile can help us to assess C sequestration potential at timescales relevant for climate change mitigation. Bioturbation, liquid phase transport, belowground C inputs, and microbial activity, are the main processes contributing to the formation of soil C profiles, and these processes are represented in models using the advection-diffusion-reaction paradigm. Based on simulation examples, and measurements from carbon and radiocarbon profiles across biomes, we found that advective and diffusive transport may only play a secondary role in the formation of soil C profiles. The difference between vertical root inputs and decomposition seem to play a primary role in determining the shape of C change with depth. Using the transit time of carbon to assess the timescales of carbon storage of new inputs, we show that very small quantities of new carbon inputs travel through the depth profile and can be stabilized for time horizons longer than 50 years. Our results imply that activities that promote C sequestration in the subsoil must take into consideration the very small quantities that can be stabilized in the long term. Therefore, promoting conservation of deep soil carbon may be more relevant for near-term climate change mitigation than promoting new carbon inputs to subsoil.

Keywords: Climate change mitigation, soil carbon sequestration, transit time, advection-diffusion-reaction, microbial decomposition, organic matter stabilization, radiocarbon

*Note to coauthors: Please add your affiliation and ORCID.
Also, please read the manuscript thinking about references to include or aspects that need more development.

Contents

1 Introduction

Soil carbon stocks below surface horizons are not only one of the largest C reservoir of the terrestrial surface, but are also relatively old as demonstrated by radiocarbon measurements (Mathieu et al., 2015; He et al., 2016; Shi et al., 2020). These radiocarbon measurements along the vertical profile have shown that the age of carbon decreases significantly with depth, indicating that carbon may be stabilized for centuries to millennia in the subsoil. It is therefore reasonable to think that soils could act as a large sink for fossil-fuel derived carbon if subsoil carbon sequestration is promoted, particularly in agricultural lands. [1] [2]

Managing soils for C sequestration purposes implies that the fate of new carbon inputs and the time this carbon remains in soils can be quantified (Crow and Sierra, 2022). Mathematical models of subsoil carbon dynamics play an important role for this purpose, and can be used to estimate the potential for subsoil carbon sequestration due to land management.

In this review, we survey the main processes that contribute to soil carbon storage and dynamics in the subsoil, with particular emphasis on mathematical models of subsoil carbon dynamics. Our guiding question is whether a process understanding of soil C movement in the vertical profile can help us to assess C sequestration potential at timescales relevant for climate change mitigation. For this purpose, we first review process understanding of subsoil C dynamics, and then review mathematical models used in the past to represent these processes. Based on this review, we show that most previous models can be generalized under one single modeling paradigm, and through examples, show the main contribution of different processes in shaping soil carbon profiles. In addition, we present a conceptual framework to assess carbon sequestration on how to assess the fate of new inputs as they move through the subsoil. We use the theoretical framework provided by the transit time distribution of carbon in compartmental systems, and discuss our results in the context of soil carbon management for climate change mitigation.

2 Processes contributing to the formation of soil carbon profiles

The accumulation of organic carbon in the vertical profile is an important part of soil formation (Jenny, 1980; van Breemen and Buurman, 1997), taking place on timescales of decades to millennia. Overall, soil carbon dynamics are determined by the gain and loss (above and belowground) of carbon inputs, and decomposition. When studying the vertical distribution of soil carbon, the depth dependence of these processes is relevant, as well as vertical transport, erosion and deposition. Vertical organic matter transport can have a major effect on the soil carbon profile and is generally caused by mixing processes and transport of mobile fractions with the liquid phase (van Breemen and Buurman, 1997; Rumpel and Kögel-Knabner, 2011). In terrestrial soils, mixing of the soil—referred to as "pedoturbation" (Hole, 1961)—can occur by several processes, including the reworking activity of soil fauna (bioturbation) and freezing and thawing (cryoturbation) (Johnson et al., 1987). Cryoturbation occurs mainly in permafrost affected soils, which cover large regions at high latitudes. In other systems however, bioturbation and liquid phase transport are the main transport processes that redistribute carbon vertically.

In layers with high organic matter concentrations, an important additional transport flux occurs that is generally ignored in soil carbon profile models. Loss of mass due to decomposition leads to downward shift of material above, while surface litter deposition continually buries older material. This causes advective downward flow of material unrelated to mixing or water movement (Ahrens et al., 2015). Kaste et al. (2007) found this process to be relevant for the vertical distribution of 210Pbex in the organic surface horizon of a podzol.

[1] Martin, Nargish, Thomas: Could you add a paragraph here on current discussions and motivations for increasing C storage in the subsoil for agricultural soils? Something related to the discussions in CarboSeq/EJP Soil would be helpful.

[2] Zhongkui and Guocheng: maybe we could also add a paragraph here about the transit time results from the GCB paper. Could you add a paragraph or a few sentences about the topic?

2.1 Bioturbation

Bioturbation is defined as the biological reworking of soils and sediments by different kinds of organisms, including plant rooting systems, and most importantly, burrowing animals (Meysman et al., 2006). Chapin et al. (2002) noted that in temperate regions the mixing activity of earthworms represents a force that is orders of magnitude larger than other geomorphic processes such as erosion. The potential effects of bioturbators on their habitat are so severe that they have been called "ecosystem engineers" (Meysman et al., 2006). The rate of soil displacement by bioturbating organisms is usually estimated by measuring deposition of mounds at the soil surface. Paton et al. (1995) reviewed a range of quantitative estimates for different organisms. They concluded that the most important animal groups are earthworms, ants, mammals, and termites, with rates of mounding that can range from 0.0063 to 27 kg m^{-2} yr^{-1} .

Soil mixing by bioturbation has a homogenizing effect on soil properties: it increases dispersal of particles, reduces concentration gradients, and destroys layering (Johnson et al., 1987). Hence, bioturbation leads to organic matter diffusion and potentially to deepening of the soil profile. However, at small spatial scales the effects of bioturbation are more complex, for several reasons: (i) Certain fractions may be transported preferentially. For example, since mixing by earthworms is mostly related to feeding, it is more likely to affect (fresh) litter rather than mineral fractions (Johnson et al., 2005). The coarsest fractions, including stones, may be completely unaffected by bioturbation. (ii) Mixing may occur more strongly in one direction than in others (anisotropic mixing). For example termites bring clay particles from considerable depths to the soil surface for incorporation into their surface mounds (Paton et al., 1995). (iii) The distance of particle translocation may be in some cases quite large compared to the scale of a single soil profile (Boudreau, 1986b).

Although the relevance of bioturbation for organic matter redistribution is well recognized (van Breemen and Buurman, 1997; Chapin et al., 2002; Hoosbeek and Scarascia-Mugnozza, 2009), very few empirical studies have been performed on its effects on the the shape of the soil C profile (Tonneijck and Jongmans, 2008; Yoo et al., 2011), particularly on long timescales. Based on micromorphological analysis and radiocarbon measurements, Tonneijck and Jongmans (2008) showed that bioturbation was the main mechanism for carbon input at depth in a volcanic ash soil, more important than liquid phase transport and root input. On shorter time scales, studies of earthworm invasions in forests have demonstrated dramatic effects on organic surface layers (Alban and Berry, 1994; Bohlen et al., 2004). For example, Alban and Berry (1994) found that increasing earthworm populations in a temperate podzol led to a reduction of forest floor mass by 85 % and disappearance of the eluviation horizon in 14 years.

2.2 Liquid phase transport

A small part of organic matter in soils is dissolved in the liquid phase. Concentrations of dissolved organic carbon (DOC) are typically so low that total organic carbon in solution is negligible compared to the immobile fraction (Michalzik et al., 2001). However, leaching and decomposition fluxes of dissolved organic matter may be important terms in shaping the dynamics of soil carbon at depth (Kalbitz and Kaiser, 2008; Kindler et al., 2011). DOC is highly relevant for the formation of the soil profile since it is subject to potentially very fast transport with downward water fluxes and represents a mechanism of organic matter input at depths well below the zone where bioturbation and root input are relevant (Rumpel et al., 2012). Furthermore, adsorption of DOC to the mineral phase is one of the main mechanisms for organic carbon stabilization and persistence (Kalbitz and Kaiser, 2008). DOC is not chemically well defined, but consists of a broad spectrum of organic substances ranging from small molecules to complex humic acids (Kalbitz et al., 2000; Michalzik et al., 2001). The biodegradability of these substances ranges over several orders of magnitude (Kalbitz et al., 2000), with more resistant compounds generally increasing with depth (Kalbitz et al., 2000; Sanderman et al., 2008).

DOC may originate from several sources, with their relative contribution being highly variable for different ecosystems (Kalbitz et al., 2000). Leaching of fresh litter contributes strongly to DOC production in the surface organic layer. However, for most plant species litter leachate is relatively labile, and thus may not contribute strongly to DOC in the mineral soil (Neff and Asner, 2001). More

complex and recalcitrant dissolved organic substances may be formed predominantly as a byproduct of decomposition, contributing more to DOC in the mineral soil.

DOC also enters the soil by throughfall (Michalzik et al., 2001), and root exudation (Neff and Asner, 2001), and it is removed from the soil solution by uptake and decomposition by microbes. A considerable part of DOC is easily degradable, but this fraction decreases strongly with depth (Kalbitz et al., 2000). Another important mechanism for DOC removal is immobilization due to interactions with the solid phase and (co-)precipitation. Through a range of chemical mechanisms, DOC is adsorbed to surfaces of minerals (particularly Al and Fe hydroxides and clay) and to a lesser extent to solid organic matter (Neff and Asner, 2001). These interactions are highly variable and depend on the chemical properties of DOC, the sorbent, and the soil solution. Furthermore, in acid soils DOC may (co-)precipitate with Al and Fe ions, which is an important process for the formation of the illuviation horizon in podzols (van Breemen and Buurman, 1997). As a result of these interactions, vertical transport of DOC is significantly lower than that of water, and DOC concentrations are often much lower in the deep soil than near the surface.

2.3 Depth dependence of organic matter input

Total litter input to soil can be divided into an aboveground fraction: leaves/needles, stems, branches, and fruits; and a belowground fraction, also referred to as rhizodeposition: root mortality, sloughing off of root tissue, and secretion of mucilage and root exudates (Nguyen, 2003). The relative distribution of the litter input over these two fractions, as well as the vertical distribution of the belowground input is highly relevant for the carbon profile. Jobbágy and Jackson (2000) found a significant relationship between vertical soil carbon distribution and plant functional type, which is partially explained by ecosystem-level root/shoot ratios and the vertical distribution of root biomass. Since net primary production (NPP) is the source of litter input, its distribution over above- and below-ground biomass is a good predictor of the relative proportions of aboveground litter fall and rhizodeposition (Raich and Nadelhoffer, 1989). For instance, herbaceous vegetation types and shrubs allocate the highest fraction of NPP belowground, and forests the lowest fraction (Chapin et al., 2002). Saugier et al. (2001) compiled NPP estimates and concluded that on average 67 % and 57 % of NPP is allocated belowground for grasslands and arctic tundra, respectively, whereas for temperate and boreal forests this fraction is 39 % and 44 %. Root to shoot biomass ratios follow a similar pattern (Jackson et al., 1996). Due to the difficulty of measuring NPP, particularly belowground, these figures should be considered carefully (Clark et al., 2001). Furthermore, plants may change their allocation pattern and rooting profile when changes in nutrient and water availability and other environmental factors occur (Jackson et al., 2000).

Decomposition dynamics of above and belowground litter differ substantially due to differences in chemical composition and environmental factors at the deposition site—at the surface or directly within the profile. Root litter has repeatedly been found to be more chemically recalcitrant than aboveground litter due to the presence of substances such as lignin, cutin, and suberin (Rasse et al., 2005). Furthermore, since root input occurs predominantly in the mineral soil, it is subject to stabilization mechanisms related to the mineral phase such as adsorption and occlusion in aggregates (Rasse et al., 2005).

Rhizodeposition is vertically distributed over the mineral soil profile and organic surface layers. Jackson et al. (2000) analysed a global data set of root distribution measurements and found that tundra, boreal forests and temperate grasslands generally have the shallowest profiles with 80–90 % of the roots occurring at the top 30 cm of the soil. Deserts and temperate coniferous forests had the deepest rooting profiles with only 50 % of the roots in the top 30 cm. Independent of vegetation type, root distribution seems to be mostly determined by soil hydrology, as demonstrated by significant relationships between annual potential evapotranspiration, precipitation, and soil texture (Schenk and Jackson, 2002a). In more water limited ecosystems, plants tend to have deeper root profiles to maximize water uptake (Schenk and Jackson, 2002b). Roots may also preferentially grow in the organic surface layer, if present, due to the high nutrient and moisture availability there (Jordan and Escalante, 1980) (Schenk and Jackson, 2002a). Although rhizodeposition and root biomass are strongly related, they may not have exactly the same vertical distribution, since not all roots contribute

equally to organic matter input. Fine roots have higher mortality rates and excrete more exudates since they play a greater role in water and nutrient uptake (Anderson et al., 2003). Hence, it is likely that organic matter input by roots is more closely related to the fine root profile, which is more shallow than the overall distribution of roots. Furthermore, radiocarbon analysis shows that also within the fine root fraction, production and mortality rates decrease with depth (Gaudinski et al., 2010).

2.4 Depth dependence of soil organic matter properties and dynamics

The chemical properties of soils change along the vertical profile (Rumpel and Kögel- Knabner, 2011; Vancampenhout et al., 2012). Most well-known are the decrease of C/N ratio, and the enrichment of ^{13}C and ^{15}N (Ehleringer et al., 2000; Nadelhoffer and Fry, 1988; Högberg, 1997). These gradients indicate a change from plant derived to more decomposed and microbial derived organic matter with depth (Rumpel et al., 2002; Rumpel and Kögel-Knabner, 2011; Baisden et al., 2002). It has been suggested that microbial residues are more effectively stabilized by organo-mineral interactions, which have been found to be an important mechanism in the deep soil (Rumpel et al., 2012).

A distinct property of most soils is the decrease of radiocarbon (^{14}C) activity with depth, indicating a higher average age of carbon since plant uptake from the atmosphere. Near the surface, average radiocarbon age is typically in the range of 1 to 100 yr, whereas in the deep soil ages of 10 000 yr or more are no exception (Mathieu et al., 2015; He et al., 2016; Lawrence et al., 2020) (Rumpel and Kögel-Knabner, 2011). Presumably, this age gradient is partially explained by slow downward transport of carbon fractions that are either very recalcitrant, or continually recycled by microbes (Elzein and Balesdent, 1995); Kaiser and Kalbitz, 2012). However, a more important cause may be decreasing average decomposition rates along the profile (Jenkinson and Coleman, 2008; Koven et al., 2013) (Persson et al., 2000). The reason for this gradient is not fully understood yet. It may be caused by the selective preservation of recalcitrant compounds combined with downward transport (Elzein and Balesdent, 1995). Also, the dominant source of organic matter in deep soils is root input, which is chemically more recalcitrant than aboveground litter (Rasse et al., 2005).

Another cause of the decreasing decomposition rates with depth is the increased occurrence of certain stabilization mechanisms. Several studies have found that organic matter in subsoils is predominantly associated with minerals (Rumpel and Kögel- Knabner, 2011; Eusterhues et al., 2003) (Rasmussen et al., 2018) or occluded within aggregates (Moni et al., 2010). A further cause of stabilization in deep soil is physical disconnection between microbes and substrates (Don et al., 2013). Most microbial activity in deep soils is located in so-called hot spots: root and earthworm channels and preferential water flow paths (e.g. cracks). Organic matter outside of these zones may be stabilized due to spatial separation from decomposers (Chabbi et al., 2009).

3 Soil carbon profile models

While the overwhelming majority of soil carbon models do not represent spatial processes (Manzoni and Porporato, 2009), a small number of models have been published that in some way account for the vertical soil carbon profile. For example, some models vertically distribute simulated total soil organic carbon or extrapolate topsoil carbon downwards using a predefined depth-function, in order to determine lateral soil carbon transport due to erosion (Rosenbloom et al., 2001; Hilinski, 2001). Several models represent carbon pools in predefined soil layers that differ with respect to physical and chemical parameters, as well as temperature, moisture, and root input (van Veen and Paul, 1981; Grant et al., 1993). In some cases heat or water transport between layers is included to account for the effects of temperature and moisture on decomposition, or to simulate leaching of mineral nitrogen (Hansen et al., 1991; Li et al., 1992). However, these models do not consider explicitly vertical transfer of organic matter between layers. A number of models of DOC dynamics have been proposed (Michalzik et al., 2003; Neff and Asner, 2001; Gjettermann et al., 2008; Brovelli et al., 2012). These models account explicitly for production and mineralization of DOC, as well as vertical transport with water flow and ad- and desorption. Transport is usually represented as advection, based on measured or simulated water fluxes. These schemes are mainly developed to reproduce DOC fluxes and concentrations at small scales, and usually require site level calibration or detailed information on soil texture.

The effects of bioturbation in terrestrial soils have been modeled in relation to transport of radionuclides (e.g. Müller-Lemans and van Dorp, 1996; Kaste et al., 2007; Bunzl, 2002) and soil formation (Kirkby, 1977; Salvador-Blanes et al., 2007). More literature exists on modelling of benthic bioturbation and its effects on chemical species in sediments at the bottom of oceans and lakes (e.g. Boudreau, 1986b; Meysman et al., 2005, 2010) (Sarmiento and Gruber, 2006; Arndt et al., 2013). Bioturbation is usually modeled as a diffusive process, although it has been shown that this approach is not generally valid (Meysman et al., 2003, 2010). Alternatively, other schemes have been proposed to represent diffusive processes, which includes both deterministic (Boudreau, 1986a, 1989) and stochastic approaches (Bunzl, 2002; Choi et al., 2002; Meysman et al., 2008).

Perhaps the first model truly aimed at dynamically simulating the soil carbon profile was developed by Kirkby (1977), as part of a soil formation model. Since then, a number of models have been developed that combine decomposition with vertical transport, represented either as diffusion (O'Brien and Stout, 1978; van Dam et al., 1997; Koven et al., 2009), advection (Nakane and Shinozaki, 1978; Dörr and Münnich, 1989; Bosatta and Ågren, 1996; Feng et al., 1999; Baisden et al., 2002; Jenkinson and Coleman, 2008), or both (Elzein and Balesdent, 1995; Bruun et al., 2007; Freier et al., 2010; Guenet et al., 2013; Koven et al., 2013). Most of these models were developed to explain measurements of carbon and tracer profiles. Increasingly, more models are now developed to represent soil carbon cycling and predict land-atmosphere carbon exchange (Jenkinson and Coleman, 2008; Huang et al., 2018; Koven et al., 2013; Ahrens et al., 2020).

3.1 A general model of soil carbon transport and decomposition with depth

The main processes involved in the formation of soil carbon profiles (bioturbation, liquid phase transport, rhizodeposition, and decomposition) are commonly represented in models using the mathematical paradigms of diffusion, advection, and reaction, respectively. It is therefore useful to conceptualize models of SOM transport and dynamics by a general paradigm expressed as

$$\frac{\partial x(d,t)}{\partial t} = \text{Diffusion} + \text{Advection} + \text{Reaction}, \tag{1}$$

where the variable x represents soil organic matter or carbon, and variable t represents time. We use here partial derivatives (the ∂ symbol) to represent the change of soil carbon with respect to time, assuming that it can also change along a variable d that denotes soil depth. Therefore, we are also interested in representing changes in x with depth; i.e. $\partial x/\partial d$. Equation 1 is a continuity equation, expressing how the conserved quantity x, which obeys mass conservation, changes continually with soil depth and time.

Our main postulate is that all models of vertical SOM transport are special cases of 1, expressing different forms of diffusion, advection and reaction. This general approach to modeling vertical dynamics has been identified previously for diverse systems such as marine organic matter (Sarmiento and Gruber, 2006) or sediments (Arndt et al., 2013).

3.1.1 Diffusion

A simple general model of soil carbon profile dynamics including only vertical diffusion and inputs can be expressed as

$$\frac{\partial x(d,t)}{\partial t} = \frac{\partial}{\partial d}\left(\kappa(d,t)\frac{\partial x(d,t)}{\partial d}\right) + I(d,t), \tag{2}$$

where $\kappa(d,t)$ is a function that represents how mass diffusivity depends on soil depth and time. Mass diffusivity is a soil property that generally does not change considerably over short timescales, and in the most simple case it can be expressed as a constant κ with no depth dependence. The function $I(d,t)$ expresses how litter and root inputs change with depth and time, and can take multiple forms depending on attributes of the vegetation such as phenology, allocation, and rhizodeposition.

Models of the form of equation 2 can only be solved (analytically or numerically) if initial conditions $x(d,0)$ are known as well as the carbon contents at the extremes of the vertical profile, between a depth at the surface d_0 and some maximum depth $d_{\max}$. Soil carbon values at these depths ($x(d_0,t)$ and

$x(d_{\max}, t))$ are called the boundary conditions, and must be known a priori in order to obtain solutions of these models.

To obtain an intuitive understanding of potential solutions to this model, it is useful to assume mass diffusivity as a constant (κ) and that inputs of organic matter to the soil are constant over time according to some function $I(d)$. Under these conditions, the soil carbon content along the profile reaches a steady-state in which it does not change over time; i.e.,

$$\frac{\partial x(d,t)}{\partial t} = 0,$$

and the steady-state carbon content along the profile $x(d)$ is the solution to the second order ordinary-differential equation

$$\frac{\partial^2 x}{\partial d^2} = -\frac{I(d)}{\kappa}. \tag{3}$$

Again, this equation can be solved using boundary conditions, integrating with respect to d to obtain the distribution of carbon content with depth $x(d)$. Equation 3 implies that the steady-state carbon content in a diffusion controlled environment is mostly defined by the relation between the depth distribution of inputs and the mass diffusivity of the soil. The vertical distribution of inputs is mostly a property of the vegetation and the rhizosphere system, while mass diffusivity is mostly a property of the soil and the organisms that act as bio-engineers.

3.1.2 Advection

The other main mathematical paradigm used to represent vertical processes in soil carbon profiles is advection; i.e., the transport of organic carbon dissolved in water. Following mass conservation, advection can be expressed as

$$\frac{\partial x(d,t)}{\partial t} = -\frac{\partial}{\partial d} f(x(d,t)), \tag{4}$$

where $f(x(d,t))$ is the flux or flow rate of mass at depth d and time t. In other words, the mass of soil carbon can only change over time due to the flow rate of the fluid along a vertical direction. If the fluid is flowing at a constant velocity v, equation 4 can be simplified to

$$\frac{\partial x(d,t)}{\partial t} = -v\frac{\partial x(d,t)}{\partial d}. \tag{5}$$

Intuitively, this implies that soil carbon is removed from a depth d at the velocity at which the fluid is passing through, and the gradient at which carbon content changes with depth. Flow velocity is determined by the combination of all the physical, chemical, and biological factors that affect water flow in saturated and unsaturated soils. Although flow velocity may not be constant in most cases, equation 5 helps to understand its role in modeling SOM transport mechanisms in soils.

To better understand the role of $f(x(d,t))$ in equation 4, it is useful to think of $x(d,t)$ as a density function that represents the mass concentration of SOM at a particular depth and time. Therefore, the total mass of carbon between two depths d_1 and d_2 at time t is given by

$$\int_{d_1}^{d_2} x(d,t)\ \mathrm{d}d.$$

Because in an advection only system the total mass between the depths d_1 and d_2 only changes due to the flux at the end points, we can assume that

$$\frac{\mathrm{d}}{\mathrm{d}t}\int_{d_1}^{d_2} x(d,t)\mathrm{d}d = f(x(d_1,t)) - f(x(d_2,t)). \tag{6}$$

The function $x(d,t)$ is not know explicitly, therefore we do not have explicit formulas for the flow rates f. Nevertheless, equation 6 helps to understand the role of the flow rate function f in equation 4; it represents the flow rate of soil carbon at any given depth and time.

3.1.3 Reaction (decomposition)

If we ignore vertical transport, soil carbon would display temporal dynamics related to the action of microorganisms and how they consume organic matter. This process of decomposition has been studied extensively, and there are hundreds of mathematical models that represent these dynamics ignoring vertical transport processes (Manzoni and Porporato, 2009). Despite the large variety of models, most of these models can be expressed in a general expression of the form (Sierra and Müller, 2015; Sierra et al., 2018)

$$\frac{\mathrm{d}\boldsymbol{x}}{\mathrm{d}t} = \boldsymbol{u}(\boldsymbol{x}, t) + \mathbf{B}(\boldsymbol{x}, t) \cdot \boldsymbol{x}(t). \tag{7}$$

This general model is expressed in vector and matrix form because it is assumed that soil organic carbon is highly heterogeneous, and different proportions decompose at different rates. Therefore, the vector $\boldsymbol{x}(t) \in \mathbb{R}^n$ represents the mass of soil carbon in n number of compartments at time t. The total mass at time t, $x(t)$, can be simply obtained as the sum of the elements of this vector, i.e. $x(t) = \|\boldsymbol{x}(t)\|$ (the vertical bars indicate a sum of the positive elements of a vector). Mass inputs to this system are represented by the vector $\boldsymbol{u}(\boldsymbol{x}, t)$, which expresses the amount of organic matter inputs that would enter each compartment. Because above and belowground litter inputs can differ in their chemical and physical properties, different proportions of the total mass may enter different compartments. In addition, the inputs may depend on the amount of carbon in particular compartments; for example, if exudation rates depend on the amount of mycorrhiza. For this reason, the inputs $\boldsymbol{u}$ are expressed as dependent on the amount of mass present in the compartments at any given time.

Rates of decomposition and transfer of carbon among compartments are expressed in the matrix $\mathbf{B}(\boldsymbol{x}, t)$ of equation 7. This matrix is called compartmental because it has important mathematical properties related to mass conservation: all diagonal elements are non-positive, all off-diagonal elements are non-negative, and the column sums are non-positive (Metzler and Sierra, 2018; Sierra et al., 2018).

Linear models such as Century and RothC as well as nonlinear microbial models such as those proposed by soil ecologists (e.g Schimel and Weintraub, 2003; Allison et al., 2010) are especial cases of the general model of equation 7 (Sierra and Müller, 2015), whose internal structure helps in the study particular aspects of the process of decomposition that are independent of vertical transport. These processes include: differences in the decomposability of different types of organic matter, organo-mineral interactions, effects of abiotic variables such as temperature, moisture, and pH on the rates of organic matter processing, interactions between substrates and microbial groups, among others.

To incorporate vertical transport processes in this model, we can assume that at any given depth d, reaction (decomposition) processes are expressed as

$$\frac{\partial x(d,t)}{\partial t} = \left\| \frac{\mathrm{d}\boldsymbol{x}(d,t)}{\mathrm{d}t} \right\| \tag{8}$$

where the sum is over all the compartment contents at any given depth and time. Notice that this expression contains all the litter inputs entering the soil, split according to the compartments at which they enter.

3.1.4 Combining transport and decomposition

In the previous sections, we analyzed the processes of diffusion, advection, and decomposition separately. Now we can combine them following the general paradigm expressed in equation 1. This general model has the form

$$\begin{aligned} \frac{\partial x(d,t)}{\partial t} &= \frac{\partial}{\partial d}\left(\kappa(d,t)\frac{\partial x(d,t)}{\partial d}\right) - \frac{\partial}{\partial d} f(x(d,t)) + \left\| \frac{\mathrm{d}\boldsymbol{x}(d,t)}{\mathrm{d}t} \right\|, \\ &= \frac{\partial}{\partial d}\left(\kappa(d,t)\frac{\partial x(d,t)}{\partial d}\right) - \frac{\partial}{\partial d} f(x(d,t)) + \left\| \left(\boldsymbol{u}(\boldsymbol{x}, d, t) + \mathbf{B}(\boldsymbol{x}, d, t) \cdot \boldsymbol{x}(d,t)\right) \right\|. \end{aligned} \tag{9}$$

Most mathematical models of vertical carbon transport and decomposition should be special cases of this equation. It can lead to very complex dynamics resulting from the simultaneous effect of physical, chemical and biological processes related to transport and decomposition.

Equation 9 cannot be solved analytically, but it can be discretized in time and space to obtain numerical solutions. The discretization approach consists of defining a fixed number k of depth intervals Δd where the solution of the partial differential equation is approximated using algebraic equations, and the system is then moved forward in time at discrete intervals Δt. Most numerical methods to approximate solutions to equation 9 would attempt to find a vector $\boldsymbol{X} \in \mathbb{R}^{k+2}$ for k depth intervals by solving a linear equation of the form

$$\mathbf{A} \cdot \boldsymbol{X} = \boldsymbol{F}, \tag{10}$$

where the matrix $\mathbf{A}$ and the vector $\boldsymbol{F}$ result from the linearization of the original system using a finite-difference method (Lanczos, 1996; LeVeque, 2007). The dimension of this system is $(k+2) \times (k+2)$, with the 2 additional dimensions incorporating information based on the boundary conditions, which must be added to the linearized system (Lanczos, 1996). Because after the discretization mass conservation must be preserved, we postulate that the new system of equations must be compartmental. In other words, a discretized system representing transport and decomposition of organic matter can be expressed as a compartmental system of the form of equation 7. There are a few examples from the previous literature that may help to confirm this assertion. For instance, Metzler et al. (2020) showed that the soil carbon module of the ELM model (Koven et al., 2013), which contains 10 discrete depth layers and 7 pools in each layer, can be approximated with a compartmental system that produces the exact same numerical solution as the original model that was developed with partial differential equations. Similarly, (Huang et al., 2018) expressed the same model of Koven et al. (2013) as a system of linear equations in matrix form and found exact approximations to the original model.

The approximation of the nonlinear model expressed with partial differential equations is possible if the system is assumed at steady-state. In the general model of equation 9, the steady state solution $x_{ss}(d)$ is obtained when $\partial x(d,t)/\partial t = 0$. At this steady-state, the amount of carbon stored in the system does not change over time and nonlinear interactions vanish. Therefore, the behavior of $x_{ss}(d)$ and a tracer such as ^{14}C, which is commonly used to parameterize SOC transport models, becomes linear with constant coefficients (Anderson, 2013). Thus, models of SOC dynamics with vertical transport can be expressed as linear systems with compartmental structure assuming the system is at near steady-state.

3.2 The constant coefficient model and its steady-state solution

Despite the generality of the model of equation (9) to represent vertical patterns of diffusion and advection, most of the models previously reported in the literature use constant diffusion and advection as well as constant decomposition and transformation rates (Table 1). Furthermore, most previous studies solve the model for the steady-state carbon content and analyze the resulting vertical patterns. Therefore, it is important to study in more detail a simplified version of the general model of equation 9 for the case of constant coefficients at the steady-state.

Assuming constant diffusion ($\kappa(d,t) = \kappa$ for all d and t), and constant flow velocity ($f(x(d,t) = v\,x(d)$, with v constant for all d and t), we can write a steady-state version of equation 9 by making the time derivative equal to zero as

$$\kappa \frac{\partial^2 x(d)}{\partial d^2} - v \frac{\partial x(d)}{\partial d} + g(d) = 0, \tag{11}$$

with $g(d)$ representing the balance between inputs and decomposition at each depth, also assuming constant decomposition and transformation rates at each depth ($\mathbf{B}(\boldsymbol{x}, d, t) = \mathbf{B}(d)$ for all $\boldsymbol{x}$, and t), and a constant vector of inputs at each depth ($\boldsymbol{u}(\boldsymbol{x}, d, t) = \boldsymbol{u}(d)$ for all $\boldsymbol{x}$ and t). Therefore,

$$g(d) = \|\boldsymbol{u}(d) + \mathbf{B}(d) \cdot \boldsymbol{x}(d)\|. \tag{12}$$

Equation 11 is a general form of a linear second order differential equation with constant coefficients, for which a numerical solution can be obtained by discretizing the system along fixed depth intervals and solving the resulting system of linear equations as in equation 10.

Two further simplified forms of the general equation can be found in the literature. The case in which advective transport is not considered relevant (e.g. O'Brien and Stout, 1978) and therefore

$$\kappa \frac{\partial^2 x(d)}{\partial d^2} + g(d) = 0, \tag{13}$$

or the case in which diffusive transport is not considered relevant (e.g. Feng et al., 1999; Baisden et al., 2002; Baisden and Parfitt, 2007)

$$-v \frac{\partial x(d)}{\partial d} + g(d) = 0. \tag{14}$$

To interpret data from pulse response experiments, some researchers have ignored the inputs and decomposition part of the model (e.g. Bruun et al., 2007) using an equation of the form

$$\kappa \frac{\partial^2 x(d)}{\partial d^2} - v \frac{\partial x(d)}{\partial d} = 0. \tag{15}$$

Models explicitly representing decomposition usually use one or three pools to represent decomposition as in most traditional first order pool models. More detailed representations of decomposition are presented in the model of Braakhekke et al. (2011, 2013), which represents five different pools, including a litter layer component clearly separating processes related to decomposition in the surface organic layer from processes more affected by vertical transport in the mineral horizons. Also, the model of Koven et al. (2013) used 7 distinct C pools: coarse woody debris, three litter pools, and three mineral soil C pools.

In the COMISSION model, not only advective DOC transport is considered, but also advective transport of litter particles similarly as in sediment models (Ahrens et al., 2015, 2020). In the latest version of the model (Ahrens et al., 2020), advective litter transfer and particle diffusion are depth dependent. The model also consider non-linear interactions among C pools, therefore it deviates from the constant linear coefficients model of equation 11 and is in better analogy to equation 9.

Table 1: Summary of models representing C dynamics along the vertical profile using the advection-diffusion-reaction paradigm.

Model/reference	Mathematical form	$d_{\max}$ (m)	Ecosystem/location	n	v	κ	Péclet number
O'Brien and Stout (1978)	Eq. 13	1.00	Managed pasture, NZ	1		13.2 $cm^2\ yr^{-1}$	0
Elzein and Balesdent (1995)	Eq. 11	1.65	Kattinkar, India	3	0.13 $mm\ yr^{-1}$	5.15 $cm^2\ yr^{-1}$	0.003
Elzein and Balesdent (1995)	Eq. 11	1.95	Pará, Brazil	3	0.34 $mm\ yr^{-1}$	16.58 $cm^2\ yr^{-1}$	0.002
Elzein and Balesdent (1995)	Eq. 11	1.63	Bahia, Brazil	3	0.48 $mm\ yr^{-1}$	5.29 $cm^2\ yr^{-1}$	0.009
Elzein and Balesdent (1995)	Eq. 11	0.52	Forest, Bezange, France	3	0.6 $mm\ yr^{-1}$	0.94 $cm^2\ yr^{-1}$	0.064
Elzein and Balesdent (1995)	Eq. 11	1.00	Forest, Marly, France	3	0.42 $mm\ yr^{-1}$	1.48 $cm^2\ yr^{-1}$	0.028
Feng et al. (1999)	Eq. 14	1.00	Oak chaparral, USA	1	1.51 $cm\ yr^{-1}$		∞
Feng et al. (1999)	Eq. 14	1.00	Pine, USA	1	1.67 $cm\ yr^{-1}$		∞
Feng et al. (1999)	Eq. 14	1.00	Ceanothus chaparral, USA	1	1.56 $cm\ yr^{-1}$		∞
Feng et al. (1999)	Eq. 14	1.00	Chamise chaparral, USA	1	1.52 $cm\ yr^{-1}$		∞
Baisden et al. (2002) [3]	Eq. 14		< 3 ky old grassland soil, USA	3	[4.0, 0.47, 0.40] $mm\ yr^{-1}$		∞
Baisden et al. (2002)	Eq. 14		200 ky old grassland soil, USA	3	[4.0, 0.49, 0.39] $mm\ yr^{-1}$		∞
Baisden et al. (2002)	Eq. 14		600 ky old grassland soil, USA	3	[3.2, 0.28, 0.43] $mm\ yr^{-1}$		∞
Baisden et al. (2002)	Eq. 14		3 My old grassland soil, USA	3	[0.5, 0.26, 0.10] $mm\ yr^{-1}$		∞
Bruun et al. (2007)	Eq. 15	0.55	Cropland, Denmark	0	0.0081 $cm\ yr^{-1}$	0.71 $cm^2\ yr^{-1}$	0.011
Baisden and Parfitt (2007)	Eq. 14	1.00	15 ky old grassland soil, NZ	3	[6.2, 0.9, 0.19] $mm\ yr^{-1}$		∞
Baisden and Parfitt (2007)	Eq. 14	1.00	200 ky old grassland soil, NZ	3	[0.6, 1.3, 0.25] $mm\ yr^{-1}$		∞
Baisden and Parfitt (2007)	Eq. 14	1.00	600 ky old grassland soil, NZ	3	[0.5, 0.5, 0.5] $mm\ yr^{-1}$		∞
Braakhekke et al. (2011)	Eq. 11	0.7	Deciduous forest, Germany	5	0.002 $m\ yr^{-1}$	0.6 $cm^2\ yr^{-1}$ [4]	0.333
Braakhekke et al. (2013)	Eq. 11	2.0	Pine forest, Netherlands	5	0.0651 $m\ yr^{-1}$	0.0852 $cm^2\ yr^{-1}$	76.402
Braakhekke et al. (2013)	Eq. 11	0.7	Deciduous forest, Germany	5	0.00137 $m\ yr^{-1}$	0.6792 $cm^2\ yr^{-1}$	0.202
Koven et al. (2013)	Eq. 13	3.8	Global, non-permafrost	7		1 $cm^2\ yr^{-1}$	0
Ahrens et al. (2015)	Eq. 11	0.9	Coniferous forest, Germany	4	NA	$3.24 \times 10^{-10}\ m^2\ s^{-1}$	NA

[3] The model considers three separate values of v for each C pool

[4] Assuming a bulk density of 1000 $kg\ cm^{-3}$

Particularly interesting is the model of Elzein and Balesdent (1995), which follows the form of equation 11 an includes advection, diffusion, and decomposition of three distinct pools. This model is rather useful because it includes a minimum of complexity to represent most relevant processes of a carbon transport model. It is also a useful model for parameterization against data on C and ^{14}C concentrations in vertical profiles.

Returning to our steady-state analysis of the constant coefficient model, we can solve the system for the first derivative and analyze individual components of this equation

$$\frac{\partial x(d)}{\partial d} = \frac{\kappa}{v}\frac{\partial^2 x(d)}{\partial d^2} + \frac{g(d)}{v}. \tag{16}$$

For the special case of one single pool with vertical root inputs represented by $u(d)$ and vertical decomposition rates by $k(d)$,

$$\frac{\partial x(d)}{\partial d} = \frac{\kappa}{v}\frac{\partial^2 x(d)}{\partial d^2} + \frac{u(d) - k(d)x(d)}{v}. \tag{17}$$

Equation 17 is very useful to analyze the shape of soil C profiles for cases in which the equilibrium assumption is reasonable. First, equation 17 shows that the vertical change of C in a soil profile is inversely proportional to the advective movement of C such as in the case of DOC transport. For large values of advection velocity (v) the rate of change of C by depth would be small and the vertical C profile would resemble a vertical line. Second, the sign of the rate of change of C by depth is mostly determined by the difference between belowground C inputs and decomposition. At depths where the decomposition flux ($k(d)$ $x(d)$) is larger than belowground inputs, the decrease of C by depth is maximum (maximum negative value). Third, the ratio between diffusion and advection velocity (κ/v), the inverse of the Péclet number (see below), influences how second order transport processes affect the shape of the rate of change of the vertical C profile (Figure 1).

In the analysis of partial differential equations, the Péclet number, defined as the ratio of advection to diffusion, plays a very important role in determining characteristics of the solution such as its numerical stability (LeVeque, 2007). In addition, the Péclet number can be used to determine the degree by which diffusion or advection may dominate the shape of a soil C profile (Figure 1).

If soil C always decreases with depth (Jobbágy and Jackson, 2000), the decomposition flux in equation 17 must be dominant across the entire soil profile so the rate of change with depth remains negative. In fact, this analysis suggest that the balance between lateral C inputs and decomposition is one of the main factors that affect the shape of soil C profiles where a continuous decrease in soil C is commonly observed.

A corollary or implication provided by equation 17 is that if the decrease in soil C with depth follows a simple exponential function, the right hand side of equation 17 must be a constant value for all depths. This situation seems unlikely given the different interacting process that occur in a soil, and in fact, mathematical functions different than the simple exponential provide the best fit to observed data (Jobbágy and Jackson, 2000).

3.3 Numerical example

We used equation 17 to investigate the role of diffusion, advection, decomposition and lateral inputs on the shape of soil carbon profiles. We chose values of κ and v within the range of values obtained in previous models (Table 1) as well as representative functions for $k(d)$ and $u(d)$ within the range of previous studies (e.g. Elzein and Balesdent, 1995; Jackson et al., 1996, 1997; Koven et al., 2013).

To investigate the effect of diffusion and advection, we ran simulations with values of $\kappa : \{0, 1, 5, 15\}$ cm^2 yr^{-1} and v : $\{0, 1, 5, 10\}$ cm yr^{-1} (Figure 2). The results show that vertical transport alone tends to create an accumulation horizon with largest concentrations of C close to the surface. This accumulation layer could be considered as a B horizon and can be the result of either advection or diffusion (Figure 2). Because in these simulations, lateral root inputs and decomposition decrease with depth (see below), there is a general trend of C concentrations to decline to values close to zero. Therefore, vertical transport do not seem to play a major role in transporting carbon below 50 cm depth within the range of advection and diffusion values used in these simulations. Only at

high advection velocities ($v = 10$ cm yr^{-1}) some carbon is transported below 50 cm depth, but this advection velocity is much higher than what has been used before in in other models (Table 1).

The first derivative of the C concentration profiles with respect to depth from these simulations (Figure 2 right panels), shows that vertical transport processes create an increase (positive derivative) in the topsoil layers (0-20 cm), and then it switches to negative derivatives for the subsoil. According to equation 17, the first derivative can only be positive if lateral root inputs and transport process dominate over the decomposition flux, which seems to be the case for the topsoil in these simulations. Below 20 cm depth, the decomposition flux dominates over all other processes making the first derivative negative although approaching zero in deeper layers. As advection velocity increased, the switch from positive to negative derivatives moved downward, indicating that the dominance of vertical transport over decomposition can be extended over a larger portion of the soil profile at very high advection velocities.

In a second set of simulations, we removed advection and diffusion ($\kappa = v = 0$) and represented lateral root inputs with the function

$$u(d) = -\beta^d \ \ln \beta. \tag{18}$$

This function predicts vertical root distributions and was originally proposed by Gale and Grigal (1987) and used by Jackson et al. (1996, 1997) to obtain vertical root distributions at the biome level. The original function predicts the fraction of root biomass for each depth, and multiplied by an average root turnover rate of 1 yr^{-1} (Gill and Jackson, 2000), gives the proportion of root inputs per depth interval $u(d)$. For the simulations, we used values of $\beta : \{0.92, 0.95, 0.98\}$ that include the observed extremes of values for shallow root systems ($\beta = 0.92$) and deep root systems ($\beta = 0.98$) (Gale and Grigal, 1987; Jackson et al., 1996).

The function used to represent decomposition rates by depth was extracted from Koven et al. (2013)

$$k(d) = k_0 \exp\left(\frac{-d}{d_e}\right), \tag{19}$$

with the maximum decomposition rate at the surface given by $k_0 = k(d = 0)$, and d_e representing the e-folding depth of decomposition rates. In our simulations, we used values of $k_0 : \{1, 0.1, 0.01\}$ yr^{-1} and a constant value of $d_e = 90$ cm (the model showed little sensitivity to different values of d_e).

The results from this second set of simulations evaluating the effect of lateral root inputs and decomposition showed that slowing down decomposition can have a significant effect on the shape of the vertical soil C profile. These results seems counterintuitive because equation 17 suggest that the negative term of the equation should be affected by larger values of $k(d)$, but because with slow decomposition higher amounts of C are obtained at steady-state, the entire term $k(d)x(d)$ is large, promoting a strong soil C gradient. The vertical distribution of root inputs has also a significant effect on the shape of the soil C profile, with shallow root inputs promoting a strong vertical gradient and deep rooting systems a more pronounced gradient with lower values of the first derivative. In this set of simulations, there is not an intermediate accumulation peak, and the first derivative is always negative, suggesting that only advective and diffusive processes can produce intermediate accumulation horizons where vertical transport dominates over decomposition.

4 Assessing C sequestration and the fate of new C inputs

4.1 Fate, transit time, and carbon sequestration in the subsoil

In the context of climate change mitigation, we are generally interested in evaluating the capacity of soils for storing carbon at relevant timescales associated with management and policy outcomes. In many cases we are interesting in comparing different soils; and in other cases, we are interested in evaluating the effectiveness of different soil management practices. In any case, we need to use appropriate metrics to evaluate this carbon sequestration potential.

If we aim at promoting soil C sequestration, it is then important to analyze the fate of new inputs entering the soil, assess for how long the new carbon remains stored, and how much warming can

be avoided while the C is stored (Sierra et al., 2021a; Crow and Sierra, 2022). For this purpose, we can use the following metrics: fate, transit time, and carbon sequestration, which are mathematically defined as follows.

For a compartmental system in equilibrium, where carbon inputs are balanced with C losses, the fate of C entering at a time t_0 can be obtained as a function that predicts the mass of C remaining in the soil at any given time $t > t_0$ (Sierra et al., 2021b)

$$\boldsymbol{M}(t) = e^{\tau \mathbf{B}}\ \boldsymbol{u}, \tag{20}$$

where $\boldsymbol{M}(t)$ is a vector with the mass remaining for each compartment. This mass remaining is related to the transit time of carbon, which is defined as the time it takes carbon atoms to pass through the entire network of compartments until C leaves the soil system (Bolin and Rodhe, 1973; Manzoni et al., 2009; Sierra et al., 2018). It can be expressed as (Metzler and Sierra, 2018)

$$f_T(\tau) = -\mathbf{1}^\top\ \mathbf{B}\ e^{\tau \mathbf{B}} \frac{\boldsymbol{u}}{\|\boldsymbol{u}\|} \tag{21}$$

Carbon Sequestration (CS) evaluates the fate of new inputs entering the soil integrated over a period of time. The amount of sequestration quantified by the CS metric depends on both the amount of inputs entering the soil and the time it takes this carbon to return to the atmosphere in the form of respiration. This amount of time is proportional to the transit time of carbon.

For a compartmental system at equilibrium, CS can be obtained as

$$\mathrm{CS}(t) = \int_{t_0}^{t} \|e^{\tau\ \mathbf{B}}\ \boldsymbol{u}\| \mathrm{d}\tau, \tag{22}$$

which is the integral of the total amount of mass remaining in the soil from a cohort of inputs entering at t_0.

If a particular transport-decomposition model can be discretized and expressed as a compartmental system, one can use equation 22 to quantify the CS of a particular soil and compare it with that of other soils or different forms of management.

Alternatively, $\boldsymbol{M}(t)$ and $f_T(\tau)$ can be obtained using impulse response experiments with existing transport models that are difficult to express as a compartmental system (Thompson and Randerson, 1999; Metzler and Sierra, 2018). The approach consists of running a model until reaching at equilibrium, and at this point add a pulse of carbon and observe the mass remaining of the pulse over time, which is an approximation to $\boldsymbol{M}(t)$. One can also observe the respiration flux after the addition of the pulse, which is an approximation to the transit time distribution $f_T(\tau)$ (Metzler and Sierra, 2018). The results from pulse-response experiments should provide very valuable information to assess the fate of new inputs entering the soil and whether they remain for relevant periods of time.

4.2 Numerical example

In the previous example, we saw that transport, decomposition, and lateral root inputs play an important role in determining the shape of soil C profiles at equilibrium. We evaluate now with an example how fast/slow transport, combined with fast/slow decomposition in soil profiles can affect the fate, transit time and carbon sequestration of a soil. Our aim is to assess the fate of new carbon inputs and whether they remain in soil for timescales relevant for climate change mitigation.

For this set of simulations, we used a Péclet number of 1 (Figure 1) so both advection and diffusion are considered equally relevant. For simulations with fast transport, the values of these coefficients were $\kappa = v = 5$, and for simulations with slow transport $\kappa = v = 0.1$ in $\mathrm{cm}^2\ \mathrm{yr}^{-1}$ and $\mathrm{cm\ yr}^{-1}$, respectively. Decomposition rates were considered fast with values of $k_0 = 1\ \mathrm{yr}^{-1}$ and slow with $k_0 = 0.1\ \mathrm{yr}^{-1}$ (Table 2). In all simulations, we considered a root profile with an intermediate value of $\beta = 0.95$, i.e. not too shallow nor too deep roots.

Simulation results showed that most C inputs entering at any given time only stay in the soil a few years, and only under slow transport and slow decomposition, some C may remain for a few decades (Figure 4, Table 2). Decomposition rates seem to play a stronger control on the fate of C inputs than

Table 2: Parameters used and results obtained for simulations evaluating the effect of transport and decomposition on the fate, transit time and carbon sequestration of new inputs. Tf–DF: transport fast, decomposition fast; Tf–Ds: transport fast, decomposition slow; Ts–Df: transport slow, decomposition fast; Ts-Ds: transport slow, decomposition slow.

	Tf–Df	Tf–Ds	Ts–Df	Ts–Ds
κ (cm^2 yr^{-1})	5.000	5.000	0.100	0.100
v (cm yr^{-1})	5.000	5.000	0.100	0.100
k_0 (yr^{-1})	1.000	0.100	1.000	0.100
β	0.950	0.950	0.950	0.950
Proportion remaining after 1 yr	0.338	0.687	0.436	0.904
Proportion remaining after 10 yr	0.000	0.040	0.001	0.411
Proportion remaining after 50 yr	0.000	0.000	0.000	0.018
Mean transit time (yr^{-1})	0.866	2.699	1.150	10.660
Median transit time (yr^{-1})	0.527	1.684	0.732	6.620
CS($t \to \infty$)	9.482	29.580	12.376	116.298

vertical transport rates. Under fast decomposition, most carbon was lost before 5 years and very small proportions travelled through the soil profile.

The transit time distribution of C through the soil profile for these different simulations showed that the large majority of C entering the soil at any given time is lost within the first year (Figure 5). Fifty percent of the C that enters the soil is lost in half a year in the scenario with fast decomposition and fast transport, while in the scenario with slow decomposition and slow transport 50% of the new carbon is lost in 6.6 years (Table 2). The slow decomposition scenarios showed a very different tail in the transit time distribution compared to the fast decomposition scenarios, with a larger proportion of carbon staying for longer times under slow decomposition. Therefore, the mean transit time is influenced by these long tails, with the mean transit time in the fast transport slow decomposition scenario of 2.7 years, and 10.6 years in the slow transport slow decomposition scenario (Table 2). Despite slow decomposition however, most of the new inputs do not stay for timescales beyond a few decades at the maximum.

5 Empirical evidence from soil profiles

The two numerical examples from the previous section suggest that (i) the change of soil C with depth is largely influenced by the difference between root inputs and decomposition, and to a lesser degree by vertical transport processes such as diffusion and advection; (ii) most new carbon inputs entering the soil do not remain stored for long timescales. In the following section, we will explore global-scale datasets of soil C profiles to test whether these theoretical model predictions can be confirmed with observations.

5.1 The shape of the vertical C profile across regions

The International Soil Radiocarbon Database (ISRaD) is a comprehensive and well curated collection of soil carbon and radiocarbon data (Lawrence et al., 2020). We used version 1.7.8 of the database and extracted information on soil C concentration with depth. Data from 600 individual profiles were grouped by region and averaged by 1 cm depth increments. Volcanic soils were treated as a separate group given their distinct vertical C profile. A cubic spline function was fitted to the average values to obtain an empirical function that interpolates C concentration for a continuum of depths, i.e. an approximation to the function $x(d)$ for each of the groups (Figure 6). [5]

Soil carbon decreased rapidly with depth in most soil profiles reaching values close to zero at 1 m depth (Figure 6), with the exception of soils from tundra/polar regions and volcanic soils, which still

[5] Sophie: Can you check if this is correct and add missing details about the grouping and how Figure 6 was obtained?

contain relatively large quantities of C at 90 cm depth. Averaged across sites, the data show very little evidence for intermediate accumulation horizons as in the case of the advection/diffusion experiments of section 3.3.

The first derivative of soil C concentrations with respect to depth ($\partial x(d)/\partial d$, Figure 7) showed no evidence of C accumulation horizons. In all cases, the first derivative was negative, indicating that soil C always decreases with depth for these aggregated groups. This is in contrast with the simulations in which advection and diffusion were manipulated in our simple model (Figure 2), where we observed a transition from positive to negative derivatives in the upper part of the soil horizon, but in agreement with the simulations in which root inputs and decomposition were controlled and vertical transport had a minor influence (Figure 3). Nevertheless, we observed for all groups a peak in the first derivative where it reaches a maximum negative value, indicating that soil C decreases more strongly at some intermediate depth between 10 and 20 cm (Figure 7). According to equation 17, a maximum negative value of the first derivative can only occur at depths where the microbial decomposition flux ($k(d)x(d)$) has its maximum value, i.e. when microbes are consuming the maximum amount of carbon possible.

The value of the first derivative had the largest values overall for volcanic soils, and the lowest values for arid soils. In both cases decomposition rates may be slow compared to other soils; in volcanic soils the presence of amorphous non-crystalline surfaces promote sorption of organic matter to minerals and therefore slow decomposition and strong C accumulation (Marin-Spiotta et al., 2011; Crow et al., 2015); in arid soils low moisture availability leads to slow decomposition rates, but also low primary productivity leads to low carbon stocks (Moyano et al., 2013; Sierra et al., 2015). Therefore, negative values of the first derivative are strongly dependent on the C stocks ($x(d)$), and to a lesser extend on the decomposition rate ($k(d)$). The decomposition rate obviously plays a major role in determine the size of the C stock in conjunction with the input fluxes at depth, but the rate of decline of C with depth is mostly influenced by the resulting C stock. In addition, the last term of equation 17 also reveals that for systems with slow advection velocities v approaching zero, small differences between lateral inputs and decomposition may be amplified. In other words, the large values of the negative derivative for the volcanic soils may be the result of very low advective movement of DOC, amplifying small differences between lateral inputs and decomposition.

Overall, the data from soil C profiles aggregated by regional groups and volcanic soils provide evidence supporting the idea that vertical transport may play a secondary role in determining the rate of soil C decrease with depth. The difference between lateral root inputs and decomposition may play a primary role in determining the shape of soil C profiles, and this difference may be amplified at low advection velocity rates. Diffusive movement of soil C seems to play a small role in these aggregated groups, something suggested by the low values of the second derivative (Figure 7); however, diffusion may have some control on the peak of C decrease found close to the surface in these profiles.

5.2 Transit times of C from vertical profiles

Using data from ISRaD and a dataset on root input profiles, Xiao et al. (2022) obtained estimates of mean ages and mean transit times for soil C profiles at the global scale. [6] The global averages revealed that mean transit times of C are always younger than the mean age of C stored at all soil depths (Figure 8). In other words, despite the C stored in the soil being hundreds to thousands of years old, the C respired is only a few years to decades old. This result is consistent with our transit time simulations that showed mean transit times of only a few years (Figure 5, Table 2). However, the actual values of mean transit time obtained from the data are actually much higher than those from the model results. This is to be expected given that the model used for the example only considered one single pool, but in reality soil carbon is highly heterogeneous and a proportion of its total cycles at much slower rates, which would contribute to higher transit times. In addition, sorption of OM to mineral surfaces may increase with depth, making the overall decomposition of C at depth more limited (Ahrens et al., 2020). Nevertheless, model simulations and observations agree in that new C inputs to soil only remain stored in timescales of years to decades.

Fast mean transit times were observed for tropical forest, grassland and cropland soils, while long

[6] Guocheng: please add missing relevant details.

transit times in the order of decades to centuries were only observed for tundra and boreal forest soils (Figure 8). These results are consistent with the idea that low temperatures and energy limitation may play a significant role in controlling the transit time of C at the biome level (Lu et al., 2018; Xiao et al., 2022), with fast transit times in warm regions and longer transit times in cold high-latitude regions.

Because transit times are directly related to Carbon Sequestration CS (equations 21 and 22), we expect only tundra and boreal forest soils to store C in the subsoil at timescales relevant for climate change mitigation, i.e. in the order of decades to centuries. In fact, previous studies have found that a large proportion of carbon used by microorganisms in the subsoil is recent and does not contribute to C stabilization in the subsoil (Balesdent et al., 2018; Scheibe et al., 2023). Therefore, we would expect lower values of CS for tropical forests, grasslands and cropland soils in comparison with boreal forests and tundra soils. However, it is important to keep in mind that productivity in these high-latitude regions is relatively low compared to temperate and equatorial latitudes. CS as defined in equation 22 accounts for this trade-off between the amount of inputs and its transit time through the soil, and it can be used to more specifically assess the climate mitigation potential of specific amounts of C added to the soil.

6 Summary and conclusions

We reviewed the main processes that contribute to the formation of soil C profiles, and the mathematical models that are used to represent them. Our main findings were: 1. The main processes that contribute to the formation of soil C profiles are root productivity and rhizodeposition, microbial decomposition, advective processes such as liquid phase transport, and diffusive processes such as bioturbation and cryoturbation. 2. These processes can be expressed in models under the general paradigm of the advection-diffusion-reaction equation, with most previously proposed models being a special case of this general paradigm. 3. Advective and diffusive processes seem to be of secondary importance in explaining the shape of vertical soil C profiles. The difference between vertical carbon inputs and decomposition seems to play a primary role in explaining the decline of soil C with depth. 4. The transit time of C is only a few years to decades in most soils, which implies that promoting the addition of new C inputs to soils would only contribute to climate change mitigation in the short term (years to decades). Carbon sequestration at longer timescales is only possible in slow cycling systems such as tundra and boreal forest soils, but primary production is relatively low in these regions.

Although soils store large quantities of C in the subsoil and this carbon is hundreds to thousands of years old, our review suggest that the new carbon the enters the soil is cycled quickly by the activity of microorganisms with relatively fast transit times. Therefore, promoting new C inputs to subsoil may not have a significant contribution to climate change mitigation as it could be inferred from carbon stocks and ages in the subsoil alone. Conservation of existing soil C stocks seems to be a more relevant and important aspect because the timescales required to form existing soil C stocks were on the order of centuries to millenia and there are important risks that through land use change, or non-sustainable agricultural practices, important portions of these existing stocks may be lost quickly. [7]

Acknowledgements

CAS would like to acknowledge financial support provided by the Faculty of Forest Sciences at the Swedish University of Agricultural Sciences, and the Max Planck Society.

[7] To all coauthors: Is there any aspect that is missing or not very well developed? What can be improved, particularly in this last section?
Also, I now there are many missing references. Can you help by indicating where important references should be added? Please include a doi for the respective reference

References

Ahrens, B., Braakhekke, M. C., Guggenberger, G., Schrumpf, M., and Reichstein, M. (2015). Contribution of sorption, DOC transport and microbial interactions to the ^{14}C age of a soil organic carbon profile: Insights from a calibrated process model. *Soil Biology and Biochemistry*, 88:390 – 402.

Ahrens, B., Guggenberger, G., Rethemeyer, J., John, S., Marschner, B., Heinze, S., Angst, G., Mueller, C. W., Kögel-Knabner, I., Leuschner, C., Hertel, D., Bachmann, J., Reichstein, M., and Schrumpf, M. (2020). Combination of energy limitation and sorption capacity explains 14c depth gradients. *Soil Biology and Biochemistry*, 148:107912.

Allison, S. D., Wallenstein, M. D., and Bradford, M. A. (2010). Soil-carbon response to warming dependent on microbial physiology. *Nature Geosci*, 3(5):336–340. 10.1038/ngeo846.

Anderson, D. H. (2013). *Compartmental modeling and tracer kinetics*, volume 50. Springer Science & Business Media.

Arndt, S., Jørgensen, B. B., LaRowe, D. E., Middelburg, J. J., Pancost, R. D., and Regnier, P. (2013). Quantifying the degradation of organic matter in marine sediments: A review and synthesis. *Earth-Science Reviews*, 123(0):53–86.

Baisden, W. and Parfitt, R. (2007). Bomb 14C enrichment indicates decadal C pool in deep soil? *Biogeochemistry*, 85(1):59–68.

Baisden, W. T., Amundson, R., Brenner, D. L., Cook, A. C., Kendall, C., and Harden, J. W. (2002). A multiisotope c and n modeling analysis of soil organic matter turnover and transport as a function of soil depth in a california annual grassland soil chronosequence. *Global Biogeochem. Cycles*, 16(4):1135.

Balesdent, J., Basile-Doelsch, I., Chadoeuf, J., Cornu, S., Derrien, D., Fekiacova, Z., and Hatté, C. (2018). Atmosphere–soil carbon transfer as a function of soil depth. *Nature*, 559(7715):599–602.

Bolin, B. and Rodhe, H. (1973). A note on the concepts of age distribution and transit time in natural reservoirs. *Tellus*, 25(1):58–62.

Braakhekke, M. C., Beer, C., Hoosbeek, M. R., Reichstein, M., Kruijt, B., Schrumpf, M., and Kabat, P. (2011). Somprof: A vertically explicit soil organic matter model. *Ecological Modelling*, 222(10):1712–1730.

Braakhekke, M. C., Wutzler, T., Beer, C., Kattge, J., Schrumpf, M., Ahrens, B., Schöning, I., Hoosbeek, M. R., Kruijt, B., Kabat, P., and Reichstein, M. (2013). Modeling the vertical soil organic matter profile using bayesian parameter estimation. *Biogeosciences*, 10(1):399–420.

Bruun, S., Christensen, B. T., Thomsen, I. K., Jensen, E. S., and Jensen, L. S. (2007). Modeling vertical movement of organic matter in a soil incubated for 41 years with 14c labeled straw. *Soil Biology and Biochemistry*, 39(1):368 – 371.

Crow, S., Reeves, M., Schubert, O., and Sierra, C. (2015). Optimization of method to quantify soil organic matter dynamics and carbon sequestration potential in volcanic ash soils. *Biogeochemistry*, 123(1-2):27–47.

Crow, S. E. and Sierra, C. A. (2022). The climate benefit of sequestration in soils for warming mitigation. *Biogeochemistry*, 161:71–84.

Don, A., Rödenbeck, C., and Gleixner, G. (2013). Unexpected control of soil carbon turnover by soil carbon concentration. *Environmental Chemistry Letters*, pages 1–7.

Elzein, A. and Balesdent, J. (1995). Mechanistic simulation of vertical distribution of carbon concentrations and residence times in soils. *Soil Sci. Soc. Am. J.*, 59(5):1328–1335.

Feng, X., Peterson, J. C., Quideau, S. A., Virginia, R. A., Graham, R. C., Sonder, L. J., and Chadwick, O. A. (1999). Distribution, accumulation, and fluxes of soil carbon in four monoculture lysimeters at san dimas experimental forest, california. *Geochimica et Cosmochimica Acta*, 63(9):1319–1333.

Gale, M. R. and Grigal, D. F. (1987). Vertical root distributions of northern tree species in relation to successional status. *Canadian Journal of Forest Research*, 17(8):829–834.

Gaudinski, J. B., Torn, M. S., Riley, W. J., Dawson, T. E., Joslin, J. D., and Majdi, H. (2010). Measuring and modeling the spectrum of fine-root turnover times in three forests using isotopes, minirhizotrons, and the radix model. *Global Biogeochem. Cycles*, 24(3):GB3029.

Gill, R. A. and Jackson, R. B. (2000). Global patterns of root turnover for terrestrial ecosystems. *New Phytologist*, 147(1):13–31.

He, Y., Trumbore, S. E., Torn, M. S., Harden, J. W., Vaughn, L. J. S., Allison, S. D., and Randerson, J. T. (2016). Radiocarbon constraints imply reduced carbon uptake by soils during the 21st century. *Science*, 353(6306):1419–1424.

Huang, Y., Lu, X., Shi, Z., Lawrence, D., Koven, C. D., Xia, J., Du, Z., Kluzek, E., and Luo, Y. (2018). Matrix approach to land carbon cycle modeling: A case study with the community land model. *Global Change Biology*, 24(3):1394–1404.

Jackson, R., Canadell, J., Ehleringer, J., Mooney, H., Sala, O., and Schulze, E. (1996). A global analysis of root distributions for terrestrial biomes. *Oecologia*, 10:389–411.

Jackson, R., Mooney, H., and Schulze, E.-D. (1997). A global budget for fine root biomass, surface area, and nutrient contents. *Proceedings of the National Academy of Sciences USA*, 94:7362–7366.

Jenkinson, D. S. and Coleman, K. (2008). The turnover of organic carbon in subsoils. part 2. modelling carbon turnover. *European Journal of Soil Science*, 59(2):400–413.

Jobbágy, E. and Jackson, R. (2000). The vertical distribution of soil organic carbon and its relation to climate and vegetation. *Ecological Applications*, pages 10(2):423–436.

Jordan, C. F. and Escalante, G. (1980). Root productivity in an amazonian rain forest. *Ecology*, 61(1):14–18. 0012-9658 Article type: Full Length Article / Full publication date: Feb., 1980 (198002). / Languages: EN / Copyright 1980 Ecological Society of America.

Koven, C. D., Riley, W. J., Subin, Z. M., Tang, J. Y., Torn, M. S., Collins, W. D., Bonan, G. B., Lawrence, D. M., and Swenson, S. C. (2013). The effect of vertically resolved soil biogeochemistry and alternate soil c and n models on c dynamics of clm4. *Biogeosciences*, 10(11):7109–7131.

Lanczos, C. (1996). *Linear Differential Operators*. Society for Industrial and Applied Mathematics.

Lawrence, C. R., Beem-Miller, J., Hoyt, A. M., Monroe, G., Sierra, C. A., Stoner, S., Heckman, K., Blankinship, J. C., Crow, S. E., McNicol, G., Trumbore, S., Levine, P. A., Vindušková, O., Todd-Brown, K., Rasmussen, C., Hicks Pries, C. E., Schädel, C., McFarlane, K., Doetterl, S., Hatté, C., He, Y., Treat, C., Harden, J. W., Torn, M. S., Estop-Aragonés, C., Asefaw Berhe, A., Keiluweit, M., Della Rosa Kuhnen, A., Marin-Spiotta, E., Plante, A. F., Thompson, A., Shi, Z., Schimel, J. P., Vaughn, L. J. S., von Fromm, S. F., and Wagai, R. (2020). An open-source database for the synthesis of soil radiocarbon data: International Soil Radiocarbon Database (ISRaD) version 1.0. *Earth System Science Data*, 12(1):61–76.

LeVeque, R. J. (2007). *Finite difference methods for ordinary and partial differential equations: steady-state and time-dependent problems*. Society for Industrial and Applied Mathematics, Philadelphia, PA. 2007061732 Randall J. LeVeque. ill. ; 26 cm. Includes bibliographical references (p. 329-335) and index.

Lu, X., Wang, Y.-P., Luo, Y., and Jiang, L. (2018). Ecosystem carbon transit versus turnover times in response to climate warming and rising atmospheric CO_2 concentration. *Biogeosciences*, 15(21):6559–6572.

Manzoni, S., Katul, G. G., and Porporato, A. (2009). Analysis of soil carbon transit times and age distributions using network theories. *J. Geophys. Res.*, 114.

Manzoni, S. and Porporato, A. (2009). Soil carbon and nitrogen mineralization: Theory and models across scales. *Soil Biology and Biochemistry*, 41(7):1355 – 1379.

Marin-Spiotta, E., Chadwick, O. A., Kramer, M., and Carbone, M. S. (2011). Carbon delivery to deep mineral horizons in hawaiian rain forest soils. *Journal of Geophysical Research: Biogeosciences*, 116(G3).

Mathieu, J. A., Hatté, C., Balesdent, J., and Parent, É. (2015). Deep soil carbon dynamics are driven more by soil type than by climate: a worldwide meta-analysis of radiocarbon profiles. *Global Change Biology*, 21(11):4278–4292.

Metzler, H. and Sierra, C. A. (2018). Linear autonomous compartmental models as continuous-time Markov chains: Transit-time and age distributions. *Mathematical Geosciences*, 50(1):1–34.

Metzler, H., Zhu, Q., Riley, W., Hoyt, A., Müller, M., and Sierra, C. A. (2020). Mathematical reconstruction of land carbon models from their numerical output: Computing soil radiocarbon from c dynamics. *Journal of Advances in Modeling Earth Systems*, 12(1):e2019MS001776. e2019MS001776 10.1029/2019MS001776.

Moyano, F. E., Manzoni, S., and Chenu, C. (2013). Responses of soil heterotrophic respiration to moisture availability: An exploration of processes and models. *Soil Biology and Biochemistry*, 59(0):72 – 85.

O'Brien, B. and Stout, J. (1978). Movement and turnover of soil organic matter as indicated by carbon isotope measurements. *Soil Biology and Biochemistry*, 10(4):309 – 317.

Rasmussen, C., Heckman, K., Wieder, W. R., Keiluweit, M., Lawrence, C. R., Berhe, A. A., Blankinship, J. C., Crow, S. E., Druhan, J. L., Hicks Pries, C. E., Marin-Spiotta, E., Plante, A. F., Schädel, C., Schimel, J. P., Sierra, C. A., Thompson, A., and Wagai, R. (2018). Beyond clay: towards an improved set of variables for predicting soil organic matter content. *Biogeochemistry*, 137(3):297–306.

Sarmiento, J. and Gruber, N. (2006). *Ocean Biogeochemical Dynamics*. Princeton University Press, Princeton.

Scheibe, A., Sierra, C. A., and Spohn, M. (2023). Recently fixed carbon fuels microbial activity several meters below the soil surface. *Biogeosciences*, 20(4):827–838.

Schimel, J. P. and Weintraub, M. N. (2003). The implications of exoenzyme activity on microbial carbon and nitrogen limitation in soil: a theoretical model. *Soil Biology and Biochemistry*, 35(4):549–563.

Shi, Z., Allison, S. D., He, Y., Levine, P. A., Hoyt, A. M., Beem-Miller, J., Zhu, Q., Wieder, W. R., Trumbore, S., and Randerson, J. T. (2020). The age distribution of global soil carbon inferred from radiocarbon measurements. *Nature Geoscience*, 13(8):555–559.

Sierra, C. A., Ceballos-Núñez, V., Metzler, H., and Müller, M. (2018). Representing and understanding the carbon cycle using the theory of compartmental dynamical systems. *Journal of Advances in Modeling Earth Systems*, 10(8):1729–1734.

Sierra, C. A., Crow, S. E., Heimann, M., Metzler, H., and Schulze, E.-D. (2021a). The climate benefit of carbon sequestration. *Biogeosciences*, 18(3):1029–1048.

Sierra, C. A., Estupinan-Suarez, L. M., and Chanca, I. (2021b). The fate and transit time of carbon in a tropical forest. *Journal of Ecology*, 109(8):2845–2855.

Sierra, C. A. and Müller, M. (2015). A general mathematical framework for representing soil organic matter dynamics. *Ecological Monographs*, 85:505–524.

Sierra, C. A., Trumbore, S. E., Davidson, E. A., Vicca, S., and Janssens, I. (2015). Sensitivity of decomposition rates of soil organic matter with respect to simultaneous changes in temperature and moisture. *Journal of Advances in Modeling Earth Systems*, 7(1):335–356.

Thompson, M. V. and Randerson, J. T. (1999). Impulse response functions of terrestrial carbon cycle models: method and application. *Global Change Biology*, 5(4):371–394. 10.1046/j.1365-2486.1999.00235.x.

Xiao, L., Wang, G., Wang, M., Zhang, S., Sierra, C. A., Guo, X., Chang, J., Shi, Z., and Luo, Z. (2022). Younger carbon dominates global soil carbon efflux. *Global Change Biology*, 28(18):5587–5599.

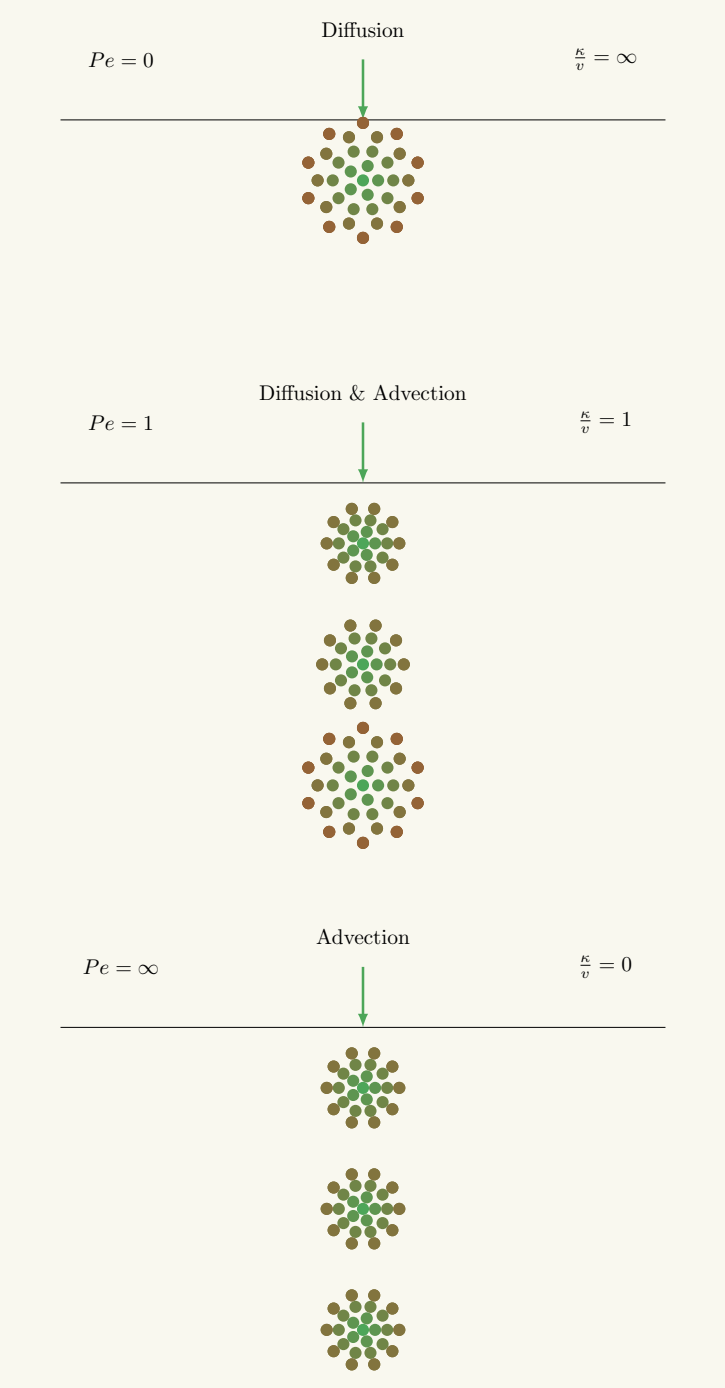

Figure 1: Schematic representation of the role of the Péclet number, which is the inverse of the κ/v ratio, on the type of vertical C transfer in a soil assuming a pulse of aboveground inputs. For a Péclet number of zero and $\kappa/v = \infty$, C entering the soil only moves due to diffusion (top); for a Péclet number and $\kappa/v = 1$, both diffusion and advection moves the carbon vertically (center); for a Péclet number of ∞ and $\kappa/v = 0$, C is only moved vertically by advective processes as in the case of DOC transport (bottom).

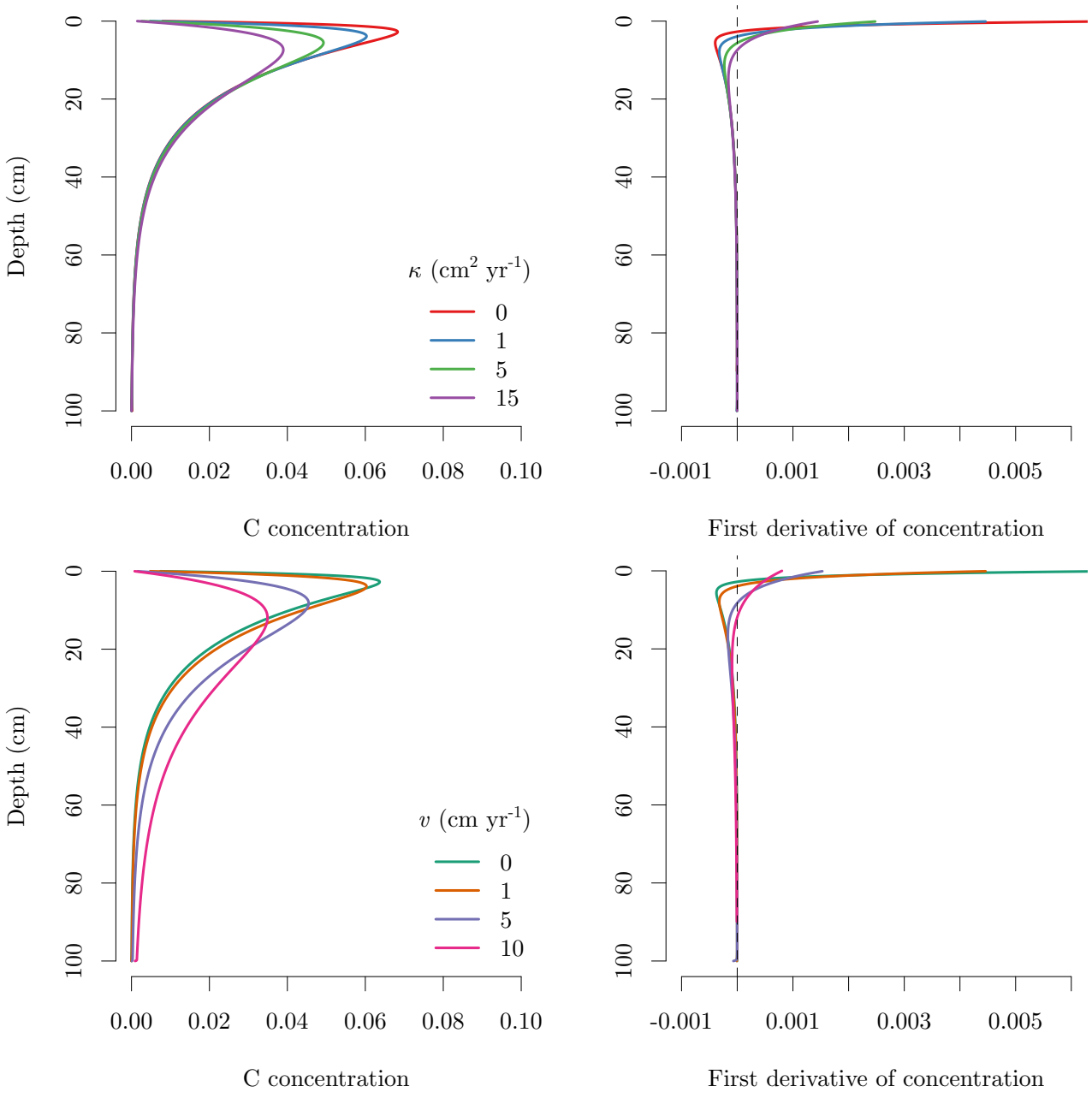

Figure 2: Numerical simulations of soil C depth profiles using the linear model with constant coefficients of equation 17. The top panels show the C concentration and the first derivative of C concentrations for different values of κ and a fixed value of $v = 1$ cm yr^{-1}. The bottom panels show C concentrations and their first derivative for different values of v and a constant value of $\kappa = 1$ cm^2 yr^{-1}.

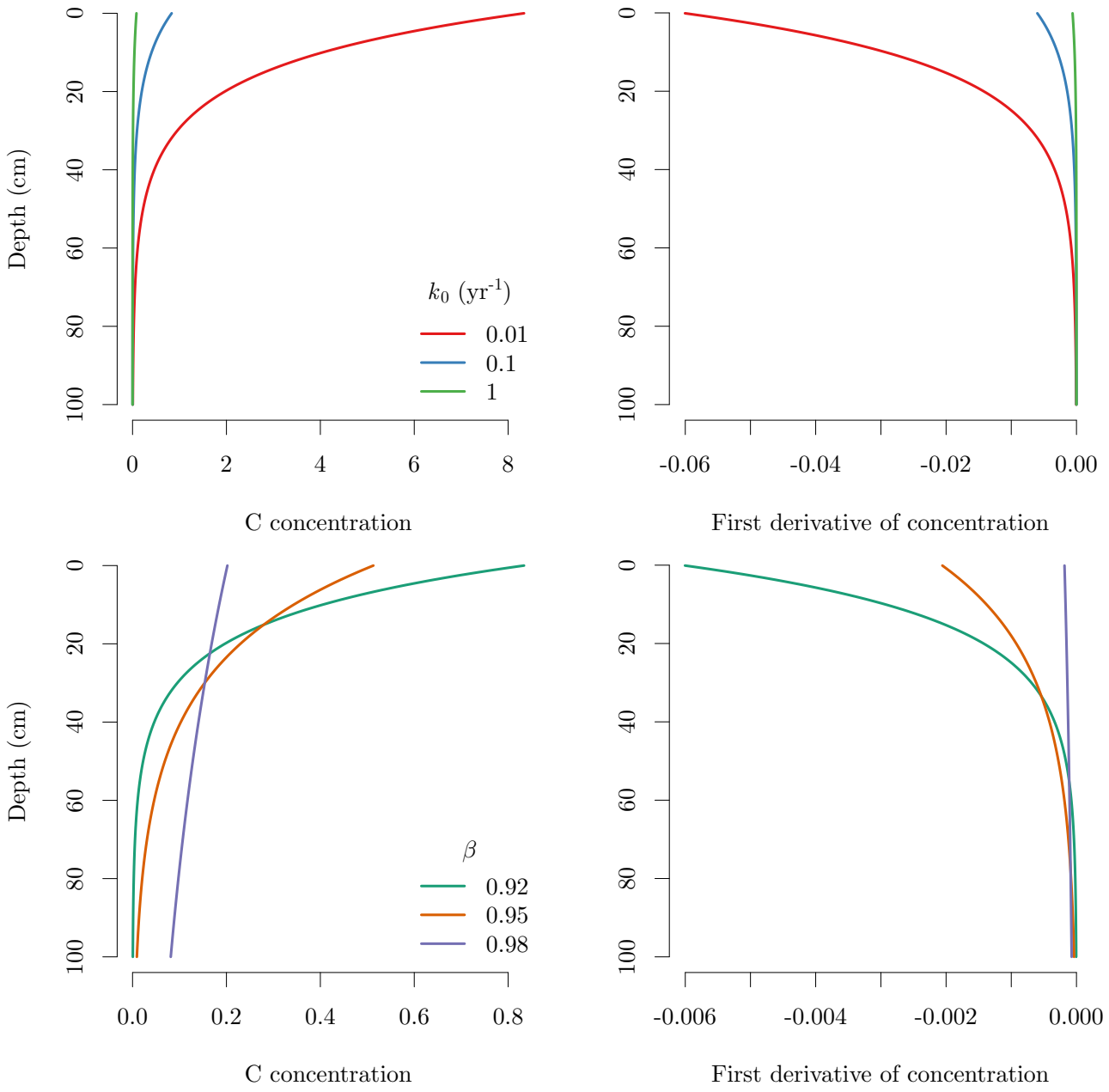

Figure 3: Numerical simulations of soil C depth profiles using the linear model with constant coefficients of equation 17. The top panels show C concentration and its first derivative with respect to depth for different functions representing decomposition rate $k(d)$ (equation 19). The different lines are the results of the model for different values of the maximum decomposition rate at the surface k_0, with the value of $k_0 = 1$ yr^{-1} representing fast decomposition and $k_0 = 0.01$ yr^{-1} slow decomposition. The lower panels represent the results of simulation for different shapes of the root input profile according to equation 18, with the parameter $\beta = 0.98$ representing deep root inputs, and $\beta = 0.92$ shallow root inputs.

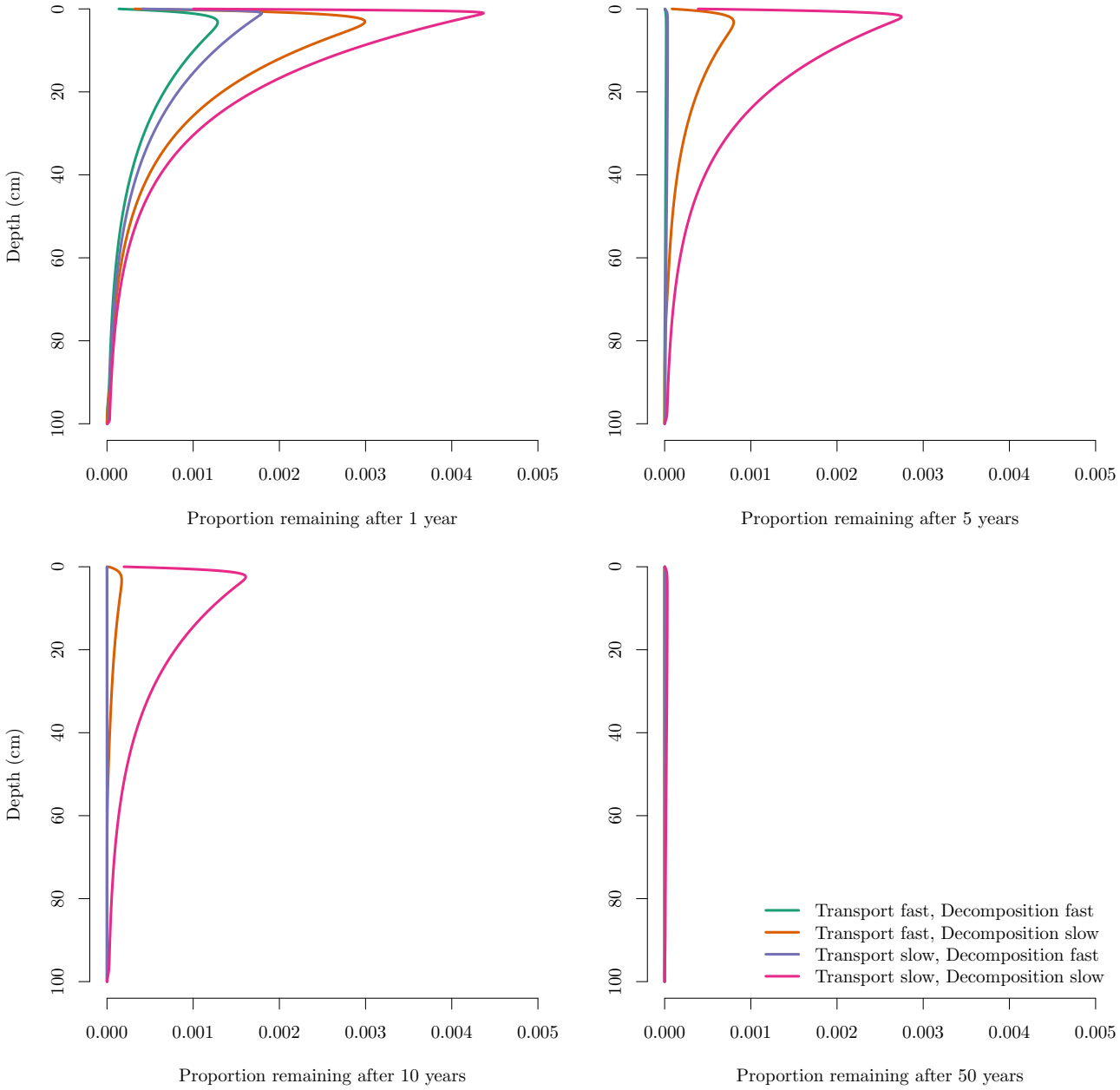

Figure 4: Proportion of C remaining in a soil profile of an amount of surface and lateral inputs entering the soil at $t = 0$ for a set of simulation experiments. After 50 years most of the carbon that entered at $t = 0$ is not present in the soil, even for the scenario with slow transport and decomposition rates.

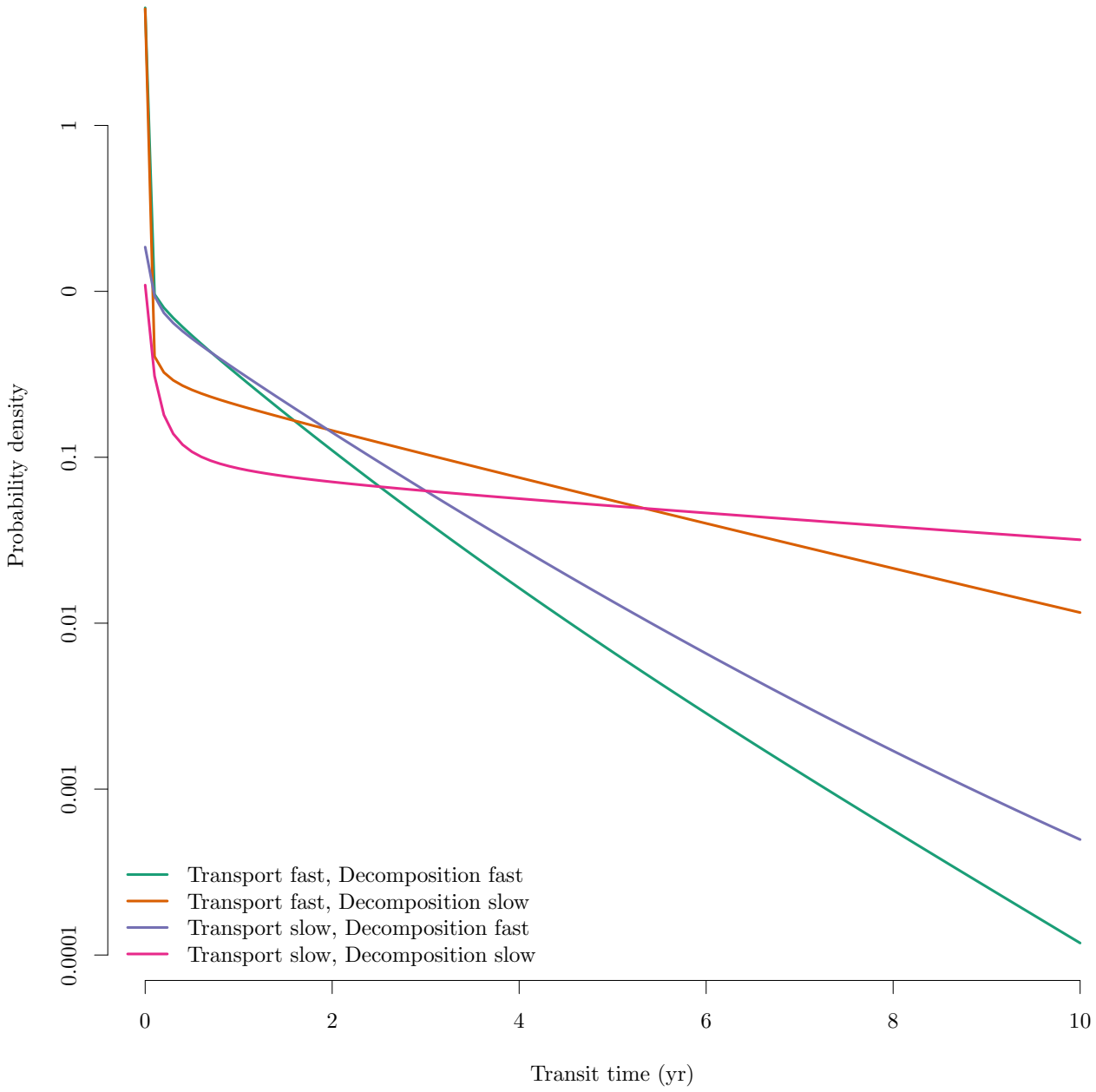

Figure 5: Transit time distributions for four different scenarios of transport and decomposition in the subsoil. These distributions represent the proportion of C leaving the soil system at different times since the C entered the soil. Note the logarithmic y axis.

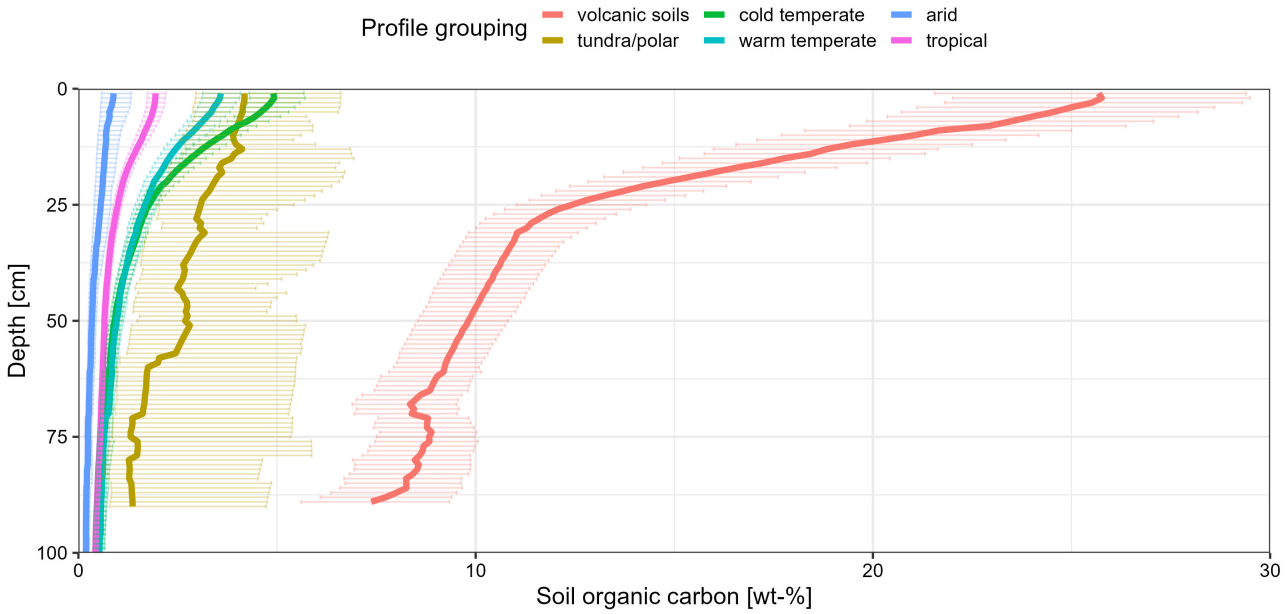

Figure 6: Soil carbon concentrations at different depths from the International Soil Radiocarbon Database, with data from 600 profiles aggregated by biogeographical regions. Thick lines for each group represent the mean across available observations and fitted to a spline curve. Horizontal lines represent standard deviation across available observations.

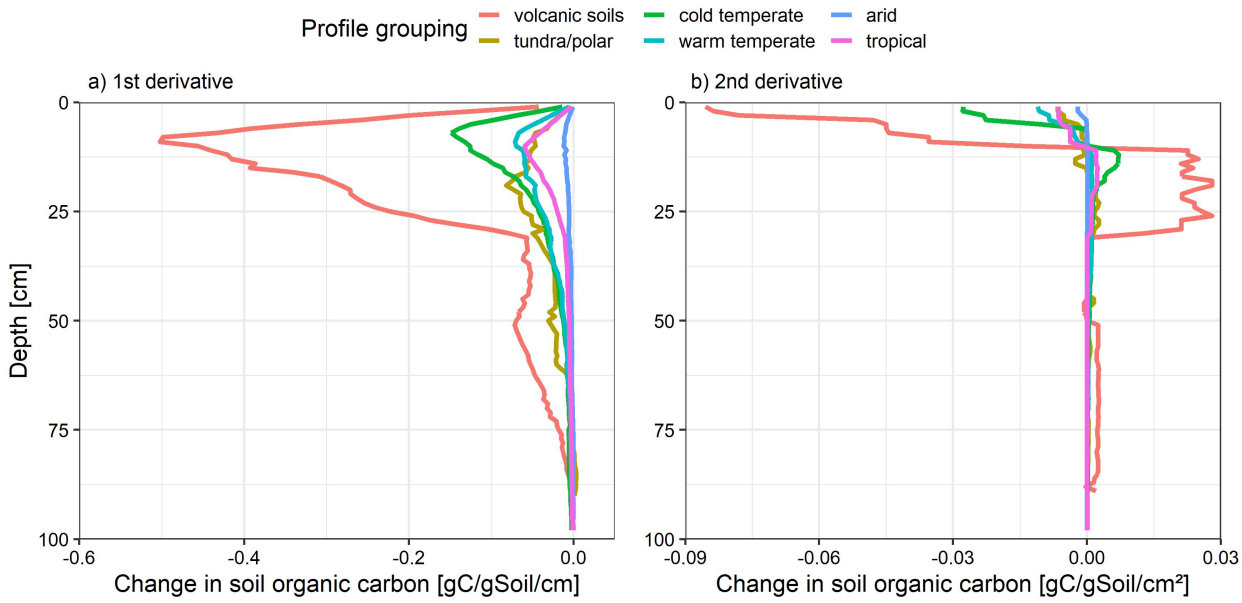

Figure 7: First and second derivative of soil C profiles extracted from ISRaD and grouped by biogeographical region, with the exception of volcanic soils.

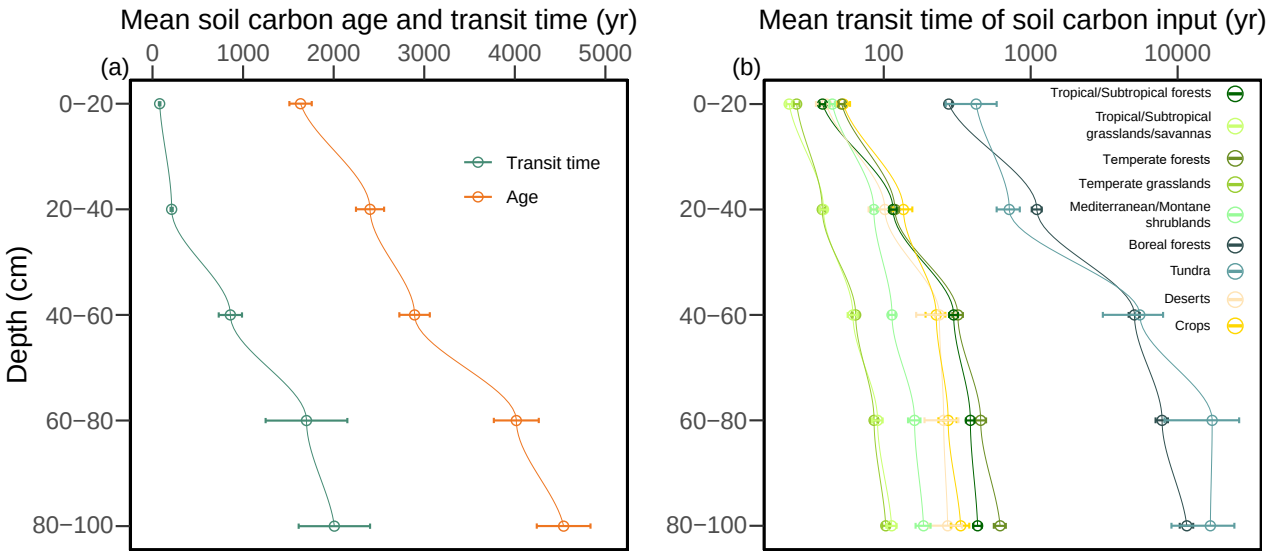

Figure 8: Estimates of mean age and mean transit time of carbon based on measurements of root inputs and soil radiocarbon obtained from ISRaD. The left panel shows global-scale average values of mean age and mean transit time. The right panel shows averages of mean transit time averaged by biome.